

A Review on TOPCon Solar Cell Technology

Hasnain Yousuf¹⁾ · Muhammad Quddamah Khokhar²⁾ · Sanchari Chowdhury²⁾ · Duy Phong Pham²⁾ · Youngkuk Kim²⁾ · Minkyu Ju²⁾ · Younhyun Cho²⁾* · Eun-Chel Cho²⁾* · Junsin Yi²⁾*

¹⁾Interdisciplinary Program in Photovoltaic System Engineering, Sungkyunkwan University, Suwon 16419, Gyeonggi-Do, Korea

²⁾Department of Electrical and computer Engineering, Sungkyunkwan University, Suwon 16419, Gyeonggi-Do, Korea

Received June 15, 2021; Revised August 27, 2021; Accepted September 3, 2021

ABSTRACT: The tunnel oxide passivated contact (TOPCon) structure got more consideration for development of high performance solar cells by the introduction of a tunnel oxide layer between the substrate and poly-Si is best for attaining interface passivation. The quality of passivation of the tunnel oxide layer clearly depends on the bond of SiO in the tunnel oxide layer, which is affected by the subsequent annealing and the tunnel oxide layer was formed in the suboxide region (SiO, Si₂O, Si₂O₃) at the interface with the substrate. In the suboxide region, an oxygen-rich bond is formed as a result of subsequent annealing that also improves the quality of passivation. To control the surface morphology, annealing profile, and acceleration rate, an oxide tunnel junction structure with a passivation characteristic of 700 mV or more (V_{oc}) on a p-type wafer could be achieved. The quality of passivation of samples subjected to RTP annealing at temperatures above 900°C declined rapidly. To improve the quality of passivation of the tunnel oxide layer, the physical properties and thermal stability of the thin layer must be considered. TOPCon silicon solar cell has a boron diffused front emitter, a tunnel-SiO_x/n⁺-poly-Si/ SiN_x:H structure at the rear side, and screen-printed electrodes on both sides. The saturation currents J_0 of this structure on polished surface is 1.3 fA/cm² and for textured silicon surfaces is 3.7 fA/cm² before printing the silver contacts. After printing the Ag contacts, the J_0 of this structure increases to 50.7 fA/cm² on textured silicon surfaces, which is still manageably less for metal contacts. This structure was applied to TOPCon solar cells, resulting in a median efficiency of 23.91%, and a highest efficiency of 24.58%, independently. The conversion efficiency of interdigitated back-contact solar cells has reached up to 26% by enhancing the optoelectrical properties for both-sides-contacted of the cells.

Key words: TOPCon Solar Cell, TOPCon solar cell fabrication, Production process of TOPCon Solar Cell, TOPCon cell efficiency progress, TCAD analysis of TOPCon solar cell

Subscript

PERC : Passivated Emitter and Rear Cell

IBC : Interdigitated back contact

TOPCon : Tunneling oxide passivated contact

LPCVD : Low pressure chemical vapor deposition

PECVD : Plasma enhanced chemical vapor deposition

APCVD : Atmospheric pressure chemical vapor deposition

1. Introduction

The efficiency of traditional manufacturing solar cells has improved by 0.5 to 0.6% per annum and is now over 22% with the passivated emitter rear cells (PERC) structure in last few years¹⁻³⁾. When the Si solar cell's efficiency approaches 23%, most of the recombination loss is due to metal contact. Therefore, contact passivation has been an enthusiastic investigation matter

of photovoltaics for several decays. Of the various resources and compositions studied, the TOPCon⁴⁾ remains the industry's greatest interest. In TOPCon design, the metal does not come into direct contact with the wafer. Alternatively, a thin tunneling oxide is applied, followed by a layer of highly doped with n or p poly silicon that contacts the metal at the ends. Behind the tunneling oxide does not affect the operation of the device, as the tunneling oxide blocks one type of carrier. Therefore, these structures are commonly referred to as the passivating contacts. SunPower Corporation was fabricating the Integrating Back Contact (IBC) cells in 2010⁵⁾, where the contact use the passivating contacts. TOPCon cell of Fraunhofer ISE with an efficiency of 25.8%^{6, 7)}, and POLO-IBC with an efficiency of 26.1%⁸⁾ were reported, where a specific surface area was 4 cm². Inspired by these excellent research advances, attempts to introduce passive contacts into industrial solar cell manufacturing are fascinating. However, there are some industry requirements to consider. Firstly, it should currently use a large silicon wafer of 156.75 × 156.75 mm², 161.7 × 161.7 mm² or more. Secondly,

*Corresponding author: echo0211@skku.edu; junsin@skku.edu

we need a high-yield poly silicon deposition system. However, there are about three different techniques considered for large scale manufacturing: low pressure chemical vapor deposition (LPCVD)⁹⁾, plasma enhanced CVD (PECVD)¹⁰⁾, inline atmospheric pressure CVD (APCVD)¹¹⁾, and sputtering¹²⁾. As far as the it knows, testing of continuous production of these deposition systems for the photovoltaic industry is still in its infancy. The third significant demand is the metallization to thin polysilicon film. High temperature screen printing is the industrial form of procedure. The challenge is to secure the thin tunnel-oxide/poly-Si layer from the annihilation of the firing-through paste at the elevated temperature. Firing from paste removes the polysilicon thin layer and introduces Ag nanoparticles into crystalline silicon that further enhance the saturation current J_o of the passivating contact region¹³⁾. The saturation current density of the metal contacts was investigated about 35 fA/cm^2 .¹⁴⁾ Polysilicon films with a thickness of more than 150 nm can withstand firing from extreme heat, on the other hand these polysilicon layers have a greater coefficient of absorption¹⁵⁾ and initiate losses in absorption. Consequently, the development of appropriate pastes from metal is currently a challenge for the photovoltaic manufacturing. Regardless of present confronts, by the interpretation of the LCOE (levelized cost of electricity), n-type TOPCon cells are favorable contestants for mainstream after PERC efficiency extend up to 23%^{16, 17)}. Current information introduces a recently produced TOPCon cell from Research and Development section with a highest efficiency of 24.58% and an open circuit voltage of 716.8 reported in journal of elsewhere, these elements are currently mass-produced by many companies¹⁸⁾.

2. Fabrication of TOPCon solar cells

The construction assembly of the cell is demonstrated in Fig. 1. It constructs with boron emitter on front side and passivating connecting layer on back side, along with fingers on both sides pasted by screen-printed system to develop bi-facial solar cell. Low amounts of oxygen required for phosphorus doped wafers, with a resistivity level of around $0.5 \text{ } \Omega\text{cm}$ to $1 \text{ } \Omega\text{cm}$. The sequence of cell construction is shown in Fig. 2. In a potassium hydroxide (KOH) solution the wafers are textured on both sides with irregular pyramids. After RCA cleaning, using a boron tribromide (BBr_3) solution the boron emitter is created in a boron diffusion furnace. By a single side etching process using hydrofluoric acid and nitric acid (HF/HNO_3) solution, the rear boron diffusion is removed. After cleaning with chemicals, a

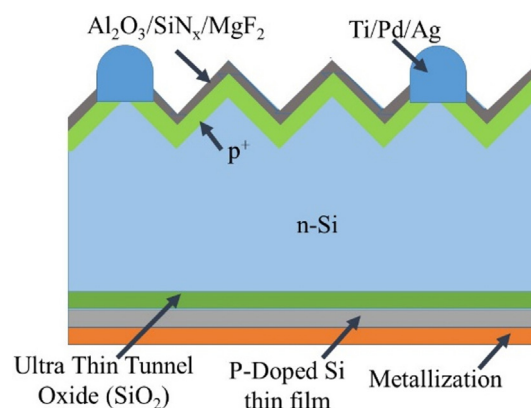


Fig. 1. The tunneling oxide passivated contact (TOPCon) solar cell of fundamental assembly



Fig. 2. Process diagram of production of TOPCon Solar Cell¹⁷⁾

tunneling SiO_x is thermally developed and a pure poly silicon layer (minimum partially poly-crystalline) is accumulated in a LPCVD system. The pure poly-silicon is doped in a phosphoryl chloride (POCl_3) diffusion furnace consequently to transform into n^+ -poly-silicon. Additionally, etching process on single side is processed to eliminate the front side covered with poly silicon. The boron emitter is passivated with film of dielectric layer, subsequently additional RCA cleaning processed, that is correspondingly work as a coating of anti-reflection layer. The back side SiO_x/n^+ -poly-silicon layer is covered with PECVD $\text{SiN}_x\text{:H}$. For metallization, an “H-metal contact” design by screen printed on both sides with 9 bus-bars, afterwards a rapid firing procedure with a highest temperature of around 760°C ¹⁷⁾. The IV curve and other important parameters are deliberate with a suitable 1-sun (1000 W/m^2) flasher instrument after construction of TOPCon solar cell.

3. Background of the Progress

The crystalline silicon solar cell has been thoroughly investigated for the previous some years. There is a high concentration of electrons in the location of the junction, thus the outcome is high loss of recombination of electrons in the solar cell, when the metal is in directly in-contact with the wafer of silicon. In the previous precedent, there were two approaches to reduce the carrier recombination of the metal precisely in contact with the silicon wafer: (1) by minimizing the interface capacity and by means of acquired smoothly doping; and (2) with employing a slight film of the passivated silicon level, to distinct the silicon wafer from the metal¹⁹⁻²¹.

The first point of the above approaches is a Passivated Emitter and Rear Cell (PERC), that is resulting from a traditional PN junction assembly, with native doping only in the emitter contact area. At present, its efficiency of current be able to attain highest as 22.8%²². The second point of the above process is Hetero-junction with Intrinsic Thin-layer (HIT) solar cell, explained by Panasonic company, these cells are presently described about 26.7% efficient^{22, 23}.

The TOPCon solar cell can additionally appear as resulting from the conventional PN junction construction, related to the advantages of the two methods presented above. In previous decades, because of admirable passivation, the TOPCon solar cell has develop most of the investigation around the scientific community. Fraunhofer Institute of Germany projected the n-type solar cell by complete distinct charge carrier selective back contact is a dual-faced connection solar cell, with a highest efficiency record about 26.7%^{22, 23}. The highest efficiency is because of the point in which the n-type silicon has a greater impurity accepted gain, and the faults in the surfaces are completely passivated. Most of the information have established that resistance of the substrate among 1 and 10 Ωcm utilized for the TOPCon solar cell that can attain more than 25% efficiency²¹. To enhance the solar cell efficiency and reserve a procedure that can endure to be augmented, the charge carrier selective contact is utilized in the projected TOPCon solar cell.

In comparison with the traditional silicon type solar cell, the TOPCon solar cell attains the subsequent purposes:^{24, 25}

1. The extreme fine layer of oxides satisfied the dangling bond that appear at the surface of the single crystal, therefore that enhance the efficiency of conversion.
2. Depending on the conductivity type of the substrate the extreme fine oxide layer allows to quick electron or hole

transfer.

3. In consequence of the extreme potential in conductivity of the heavily doped poly silicon, the resistance of the junction can be decreased and the current output could be improved.

4. TOPCon Solar Cell Structure

Fig. 1 show a fundamental layout of the TOPCon solar cell, mostly produce with a PN junction on the substrate of an n-type material^{21, 26}.

The cell is passivated by an Aluminum oxide (Al_2O_3) fine layer on the surface of the P-type material, and is contains of a very fine layer about 2 nm Silicon dioxide (SiO_2) tunneling layer and a strongly doped poly silicon film on the surface of N-type material²⁷. The major characteristics of the TOPCon solar cell is passivation on surface by the tunneling oxide film, and the selective contact to attain an incredibly minimal amount of recombination from intensely doping of poly silicon layer. To allow most of the carriers to tunnel, the tunneling SiO_2 layer needs to be thin enough for transport, however at the same moment, its field effect can avoid the minority carriers from transmitting²⁸. The characteristics of passivation of the intensely doped poly silicon layer is diverse by attuning the rate of hydrogen concentration by physical vapor deposition (PVD), for example atomic layer deposition (ALD) or sputtering, or chemical vapor deposition (CVD), such as plasma enhanced chemical vapor deposition (PECVD), or low pressure chemical vapor deposition (LPCVD). The intensively doped poly silicon layer reveals decent quality of passivation, because of the huge quantity of hydrogen atoms in the poly silicon layer²⁹.

5. Process of TOPCon Solar Cell

5.1 Ultra-Thin Oxide Layer

Operative methods for developing extreme fine layers of oxide for the TOPCon solar cell is about 1.4 to 1.5 nm comprise: thermal oxidation, wet chemical dipping, and ultra violet ozone cleaning (UV/O_3) processing. As well as, the simplest method to produce the fine layer of oxide is wet chemical dipping in the solution of acidic mixture at more than 90°C temperature. The process of thermal oxidation can be additionally separated into wet and dry oxidation from oxygen, as per the utilization of oxidizing environment. Pure and dry oxygen used for dry

oxidation from oxygen as an oxidizing atmosphere, and to form the oxide film, at high temperatures oxygen reacts directly with hydrazine gas. The moist oxygen is an extreme clear vapor of pure water as an oxidizing atmosphere, and to form the oxide film from the molecules of water and oxide on the surface reaction. Generally, the rate of oxidation for dry oxygen oxidation is lower than that of moist oxygen^{24, 27}.

5.2 Poly silicon Doped Film

The massive doping of poly silicon layer is created by 1) by utilizing LPCVD accumulating a silicon layer, reconciliation with additional ion doping, or 2) by employing PECVD precisely consigning a layer of silicon doping film.

5.3 TOPCon cell efficiency progress

The TOPCon solar cell efficiency progress is explain in two categories one is the laboratory scale and other is commercial

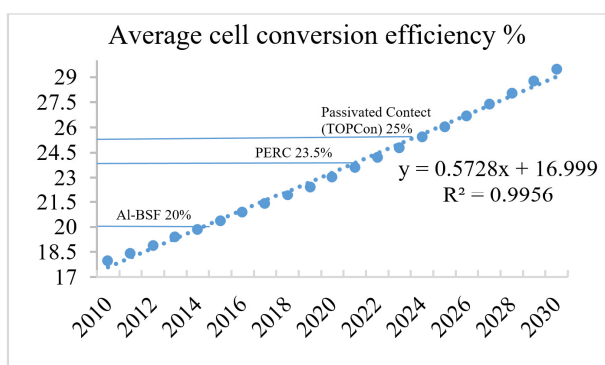


Fig. 3. Annually increment in efficiency of different solar cell technologies

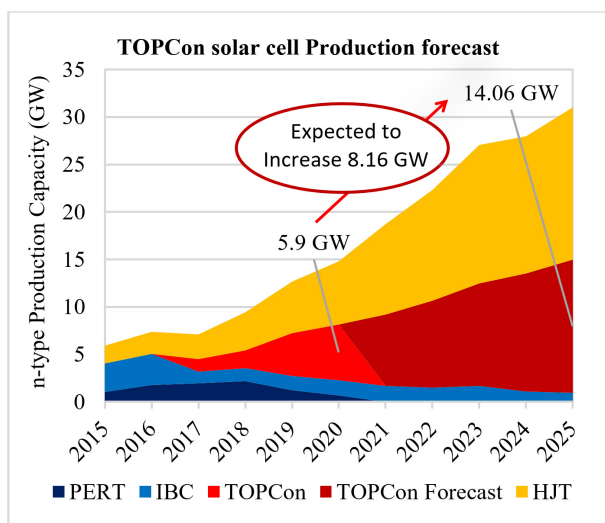


Fig. 4. TOPCon solar cell production forecast^{30, 31)}

scale efficiency. The TOPCon solar cell efficiency was reported at laboratory scale on first and second quarter of 2013 about 21.8% and 22.9%, respectively, and in the third and fourth quarter of the same year the efficiency is improved and reported about 23.6% and 23.9%, respectively. In 2014 the efficiency of TOPCon solar cell was improved to 24.3%. In the last quarter of 2015, the efficiency was reported about 25.1%. In the laboratory scale the TOPCon solar cell got efficiency about 25.8% which is reported on 2017 by the Fraunhofer ISE as shown in Fig. 5. In the commercial scale the efficiency is reported in 2017 about 22.2% which was further improved to 23.2% on 2018. The scale of the efficiencies reach higher than before and got 23.3% on 2019 which if further enhanced on 2020 and stretched at 23.6% efficiency at the commercial scale. The conversion efficiency of N-type mono-crystalline based bifacial TOPCon solar cells had reached to 25.09%, which is the first crystalline silicon solar on a commercial size wafer exceeded the efficiency of 25% as shown in Fig. 3 and expected more than 28% after the year 2028. The efficiency is enhanced as the passivation technology improve and expected to increase the TOPCon solar cell production from 5.9 GW on 2020 to 14.06 GW on 2025 as described in the Fig. 4. The production capacity was expected to more than 8.16 GW³⁰⁾.

5.4 Loss factor analysis

The loss factors are classifying in 4 categories by bulk limit, optical, recombination and resistance loss. The bulk limit is recorded as 33% on which 5.35% loss due to bulk J_0 at 10 fA/cm² and efficiency reduce to 27.6% as shown in Fig. 6 (a & b) at point 1. The second factor is optical loss which is cause by the shading 0.65%, front reflection 0.38% and escape loss 0.02% that minimize the efficiency at 26.95%, 26.75% and 26.55%

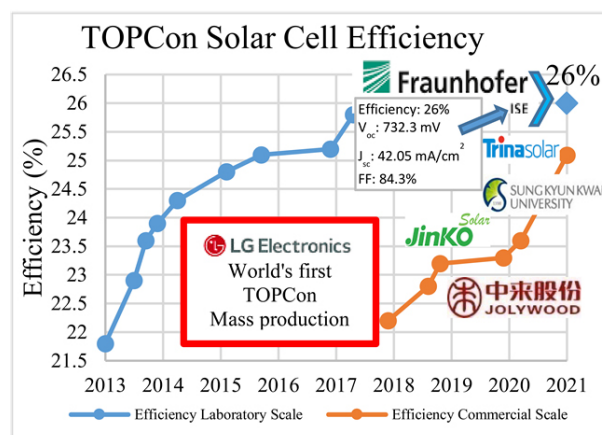


Fig. 5. Progress on TOPCon solar cell efficiencies

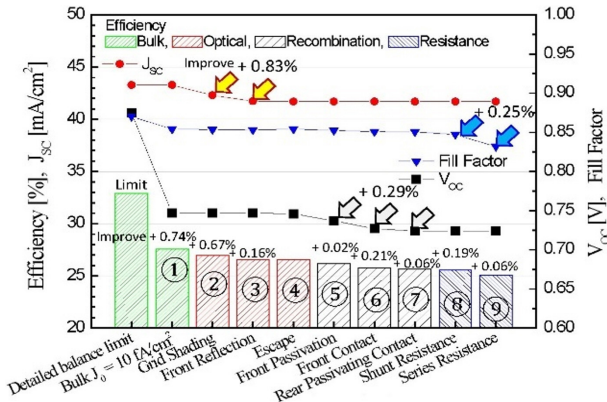
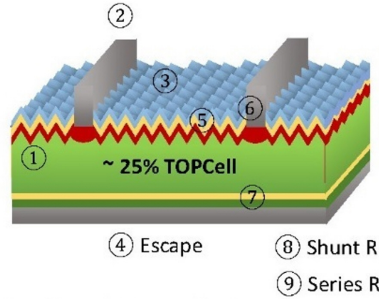


Fig. 6. (a) Loss factor analysis of bulk, optical, recombination and resistances.

J_{sc} (mA/cm ²)	V_{oc} (V)	FF (%)	Eff. (%)
41.67	0.724	83.20	25.10



Detailed Balance Limit

(Radiative & Auger Recombination)

Silicon $E_g = 1.125$ eV (@298.15 °K)

Thickness = 170 μ m

J_{sc} (mA/cm ²)	V_{oc} (V)	FF (%)	Eff. (%)
43.25	0.875	87.01	32.92

Fig. 6. (b) TOPCon Solar cell structural layout of loss factors

respectively which is shown in Fig. 6 (a & b) at point 2, 3 & 4. The third factor is the recombination loss that cause by the front passivation 0.37%, front contact 0.40% and rear passivation contact 0.11% that also lower the efficiency to 26.18%, 25.78% and 25.66% as described in Fig. 6 (a & b) at point 5, 6 and 7. The last loss factor is due to electrical resistance which is shunt resistance 0.10% and series resistance 0.46% that cause reduction in efficiency to 25.56% & 25.10% as revealed in the Fig. 6 (a & b) at points 8 & 9. The analysis of efficiency loss factor is described in Table 1 by the current density (mA/cm²), open circuit voltage V_{oc} (v), fill factor FF (%) and the final efficiency.

5.5 TCAD analysis of bifaciality and conversion efficiency with n-type TOPCon solar cell

The n-type TOPCon solar cell bifaciality and conversion efficiency is inspected by optimizing the finger width of rear-side contact. The TCAD analysis is conducted by changing the rear side finger width from 25 μ m to 1200 μ m and the efficiency on front & back side is observed and also bifaciality is calculated by dividing rear side efficiency to the front side efficiency. The efficiency is recorded at 25 μ m rear finger width as 23.01% from front side and 20.83% from the rear side, the bifaciality at this width comes to be 90.53%. As the width of the rear side finger increase the efficiency of rear side of the cell drops significantly but the efficiency of front side of the cell increase slightly. The rear side finger width at 1200 μ m, the efficiency of rear side of

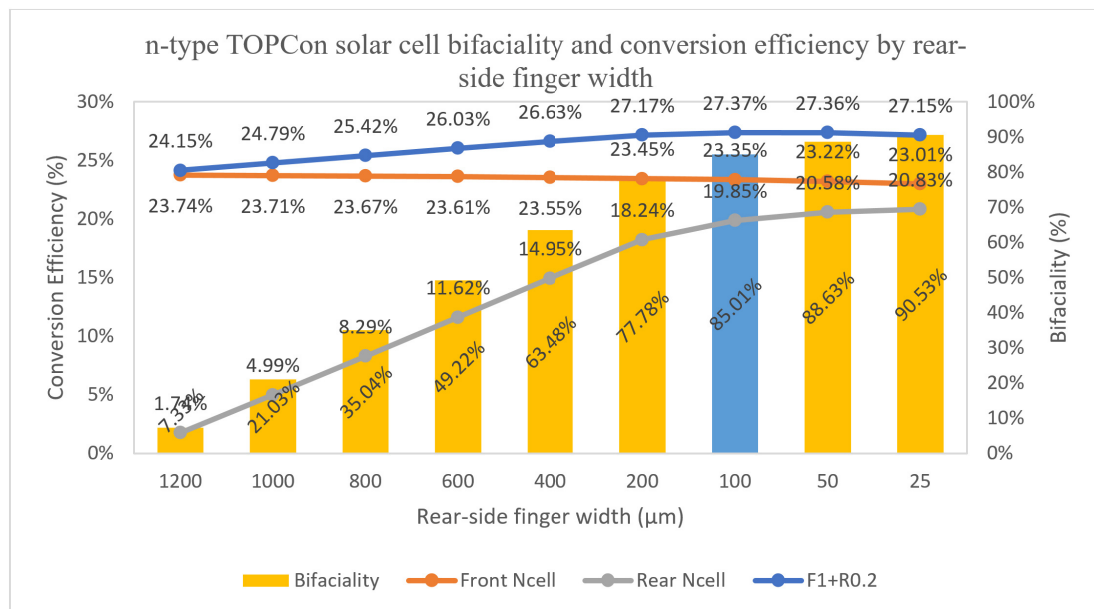


Fig. 7. TCAD analysis of bifaciality and conversion efficiency with n-type TOPCon solar cell⁽³³⁾

Table 1. Analysis of efficiency loss by material

		Cell Structure	Unit	Value	Remark	J _{sc} (mA/cm ²)	V _{oc} (V)	FF (%)	Eff. (%)	Eff. Loss (%)
SRH Bulk	①	Bulk J ₀	fA/cm ²	10	ITRPV 2019 Report	43.25	0.747	85.42	27.60	5.32
Optical Loss	②	Shading	%	2.25	Finger Width = 20 μm, Thickness = 20 μm, # of Finger = 190 ea Dual printing, Busbar = 0.3 mm (12BB), Reflected Absorption Grid	42.28	0.747	85.34	26.95	0.65
	③	Front Reflectance	%	2.26	Textured + Boron emitter + Multi Layer ARC	41.70	0.747	85.30	26.57	0.38
	④	Escape	%	0.07	Absorption missing at longwave length	41.67	0.746	85.41	26.55	0.02
Recombination Loss	⑤	Front Passivation	fA/cm ²	4.4	J _{0, full surface} = 4.5 fA/cm ² (@200 Ω/sq.) Textured + Boron emitter + Passivation with Single ARC	41.67	0.737	85.24	26.18	0.37
	⑥	Front Contact	fA/cm ²	6.89	J _{0, full contact} = 300 fA/cm ² , (@40 Ω/sq.) Contact Fraction = 2.30% (dual printing)	41.67	0.727	85.09	25.78	0.40
	⑦	Rear Passivating Contact	fA/cm ²	2.5	J _{0, full contact} = 2.5 fA/cm ² Polished + Oxide + Poly-Si (Optimized Process with SiNx Coating)	41.67	0.724	85.06	25.66	0.11
Electrical Loss	⑧	Shunt Resistance	Ωcm ²	4000	Selective emitter (200 Ω/sq. / 40 Ω/sq.)	41.67	0.724	84.73	25.56	0.10
	⑨	Series Resistance	mΩcm ²	290.9	Wafer resistivity = 5 Ωcm, Contact Resistivity = 1.5 mΩcm ²	41.67	0.724	83.20	25.10	0.46

the cell drop up to 7.33% and the front side efficiency of the cell upsurge to 23.74% and the bifaciality is calculated as 1.74% due to low efficiency of rear side of the cell. As the rear side efficiency is dropped by increasing the rear side finger width and front side efficiency is increase when the rear side width is increase, so, we can identify the optimize value of the rear side finger width using F1+R0.2. Which means that sum up the 100% efficiency value from the front side and 20% efficiency value from the rear side efficiencies. The optimum value of the rear side finger width is 100μm on which the rear side efficiency is 19.85% and front side efficiency is 23.35% and the optimum efficacy on both side is 27.37% get by F1+R0.2 as shown in the Fig. 7³³.

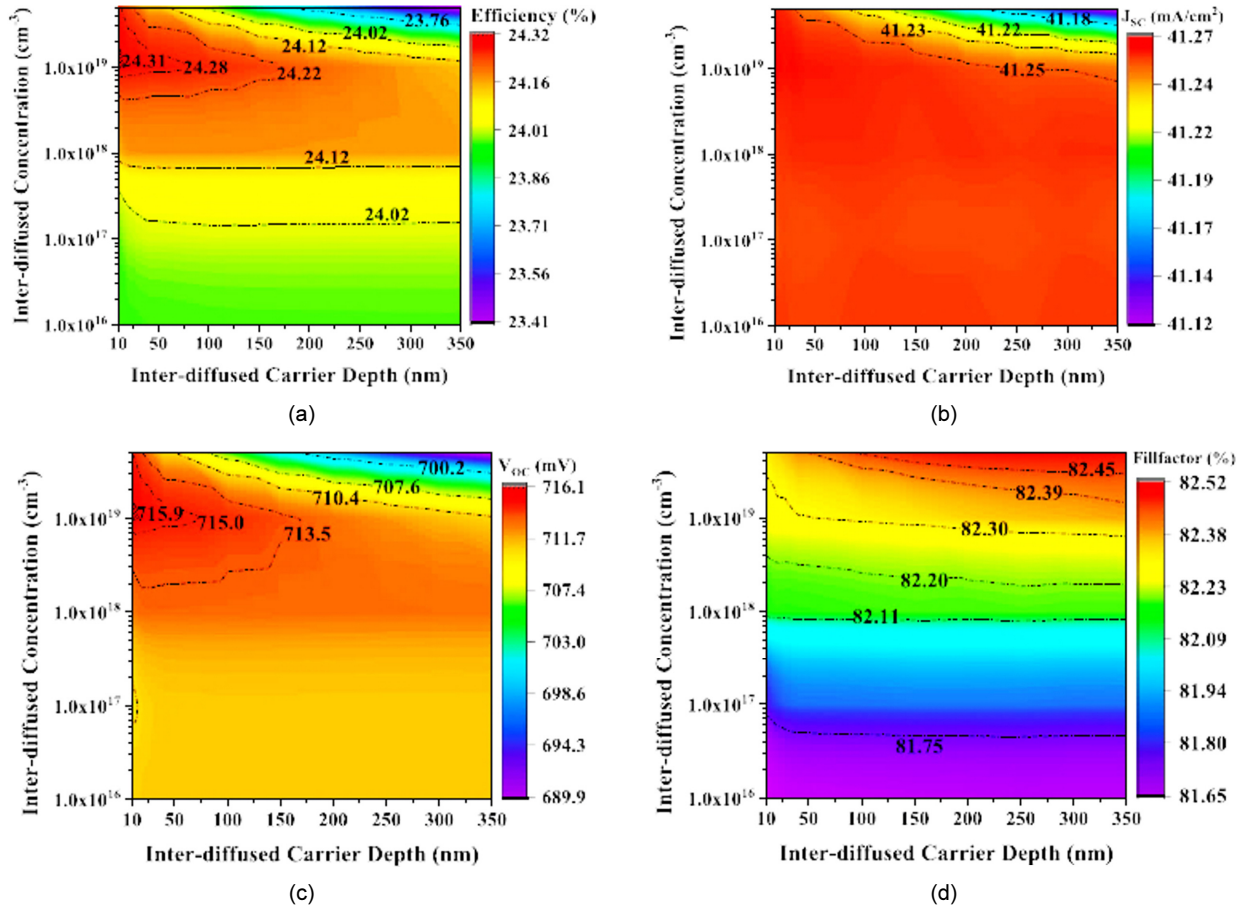
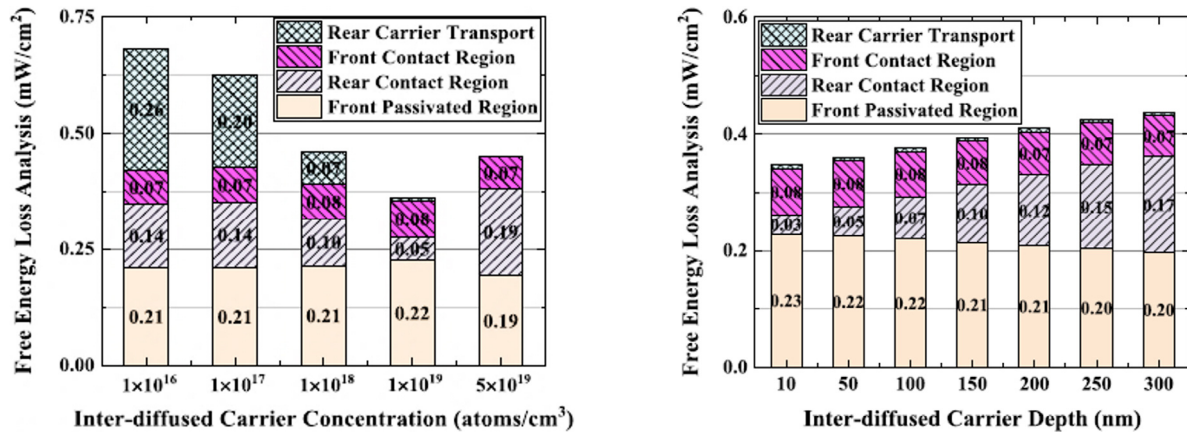
5.6 Analysis of interfuse concentration

A contour graph is plotted between Inter-diffused carrier depth and inter-diffused concentration over various parameter like efficiency (%), current density (mA/cm³), open circuit voltage V_{oc} (mV) and fill factor FF (%) as shown in Fig. 8. If the inter-diffused carrier depth is increased at same inter-diffused carrier concentration the efficiency will decreased. A high efficiency of 24.31% was obtained for the inter-diffused carrier concentration of 1×10¹⁹ atoms/cm³ at the depth of 10 nm as shown in Fig. 8(a). The current density decreases at the same inter-diffused carrier concentration when the inter-diffused

carrier depth increased. So, at low depth high current density will be obtain at low concentration as shown in Fig. 8(b). A highest open circuit voltage V_{oc} of 715.9 mV was obtained for the inter-diffused carrier concentration of 1×10¹⁹ atoms/cm³ at the depth of 10 nm as shown in Fig. 8(c). A fill factor FF (%) of 82.25% was obtained at highest efficiency for the inter-diffused carrier concentration of 1×10¹⁹ atoms/cm³ at the depth of 10 nm as shown in Fig. 8(d). The loss increases as the depth increases. The rear contact loss increases from 0.03 mW/cm² to 0.17 mW/cm² for an increase in inter-diffused depth from 10 nm to 350 nm. The impurity concentration was varied from 1×10¹⁶ atoms/cm³ to 5×10¹⁹ atoms/cm³, and the depth was changed from 10 nm to 350 nm in the TCAD tool as shown in Fig. 9³³.

6. Conclusions

In the advancement of TOPCon solar cells, it was contributory to utilize a sequence of trail tests and expounded investigation for attaining an autonomously inveterate successive efficiency of 24.58%. The stated efficiency is on larger wafer comprising bus bars and metal fingers, complete enlightenment, and fictitious with industrial manufacturing equipment. The review demonstrates that losses of recombination in the emitter, comprising its bulk, surface and metal contacts are restraining the implementation of the device, although the rear passivating contact has less J₀ of

Fig. 8. Analysis of interdiffusion concentration³³⁾Fig. 9. Free energy loss analysis (FELA) using TCAD analysis³³⁾

not more than 7 fA/cm², with the 94% non-metallized portion with $J_0 = 3.4$ fA/cm² in addition to 6% metallization section with $J_0 = 50.7$ fA/cm². It is accomplishing that enhancing the emitter and its metallization yet accepts a great ability for more improvements in efficiencies. This could be complete by advance progress of a traditional emitter construction and its metallization of paste, or by substituting it with a translucent passivating

contact. In this review, abridging the performance of poly silicon passivating contacts, in addition to emerging a blatant passivating contact that is scientifically practicable, are currently highest imperative work in silicon photovoltaic investigation and progress. The solar industry is dominated by crystalline silicon solar cells. While interdigitated back-contact cell show the greatest efficiency, double-sided contacted cells are less

complex and the recommended choice for industrial production. Avoiding the front side layer that providing lateral charge carrier transportation which is the key to the outstanding opto-electrical characteristics of the bi-directional cell. These consequences give a conversion efficiency of 26.0%. Unlike standard industrial cells which have a p-n junction at the front, the back of this cell has a p-n junction in the form of a full-surface passivation contact of polysilicon. Detailed analysis of power loss shows that these cells balances the electrons and hole transport losses, as well as typical transport losses and recombination losses. Systematic simulation studies have established some basic design rules for future silicon solar cells with efficiencies in excess of 26%, demonstrating the potential and superiority of these rear junction solar cells³²⁾.

Acknowledgment

This work was supported by the Korea Institute of Energy Technology Evaluation and Planning (KETEP) grant funded by the Ministry of Trade, Industry & Energy (MOTIE) of the Republic of Korea (20203040010320) and (20183010014270).

References

- Hermle, M., "Silicon solar cells-current production and future concepts," Fraunhofer Institute for Solar Energy Systems ISE (2017).
- Stenzel, F., Lee, B.G., Cieslak, J., Schwabedissen, A., Wissen, D., Geißler, S., Rudolph, T., Faulwetter-Quandt, B., Hönl, R., Wasmer, S., Bakowskie, R., "Exceeding 23% and mass production of p-Cz Q. ANTUM bifacial solar cells, 36th European Photovoltaic Solar Energy Conference and Exhibition, pp. 96-99 (2019).
- Rahman, M.Z., "Advances in surface passivation and emitter optimization techniques of c-Si solar cells," *Renewable and Sustainable Energy Reviews*, Vol. 30, pp. 734-742 (2014).
- Feldmann, F., Bivour, M., Reichel, C., Hermle, M., Glunz, S.W., "Passivated rear contacts for high-efficiency n-type Si solar cells providing high interface passivation quality and excellent transport characteristics," *Solar energy materials and solar cells*, Vol. 120, pp. 270-274 (2014).
- Cousins, P.J., Smith, D.D., Luan, H.C., Manning, J., Dennis, T.D., Waldhauer, A., Wilson, K.E., Harley, G., Mulligan, W.P., "Generation 3: Improved performance at lower cost," 35th IEEE Photovoltaic Specialists Conference, pp. 000275-000278, IEEE (2010).
- Richter, A., Benick, J., Feldmann, F., Fell, A., Hermle, M., Glunz, S.W., "n-Type Si solar cells with passivating electron contact: Identifying sources for efficiency limitations by wafer thickness and resistivity variation," *Solar Energy Materials and Solar Cells*, Vol. 173, pp. 96-105 (2017).
- Green, M.A., Hishikawa, Y., Dunlop, E.D., Levi, D.H., Hohl-Ebinger, J., Ho-Baillie, A.W., "Solar cell efficiency tables (version 51)," *Progress in Photovoltaics: Research and Applications*, Vol. 26, No. 1, pp. 3-12 (2018).
- Haase, F., Hollemann, C., Schäfer, S., Merkle, A., Rienäcker, M., Krügener, J., Brendel, R., Peibst, R., "Laser contact openings for local poly-Si-metal contacts enabling 26.1%-efficient POLO-IBC solar cells," *Solar Energy Materials and Solar Cells*, Vol. 186, pp. 184-193 (2018).
- Stodolny, M.K., Lenes, M., Wu, Y., Janssen, G.J.M., Romijn, I.G., Luchies, J.R.M., Geerligs, L.J., "n-Type polysilicon passivating contact for industrial bifacial n-type solar cells," *Solar Energy Materials and Solar Cells*, Vol. 158, pp. 24-28 (2016).
- Nandakumar, N., Rodriguez, J., Kluge, T., Große, T., Fondop, L., Padhamnath, P., Balaji, N., König, M., Duttagupta, S., "Approaching 23% with large-area monoPoly cells using screen-printed and fired rear passivating contacts fabricated by inline PECVD," *Progress in Photovoltaics: Research and Applications*, Vol. 27, No. 2, pp. 107-112 (2019).
- Merkle, A., Seren, S., Knauss, H., Min, B., Steffens, J., Terheiden, B., Brendel, R., Peibst, R., "Atmospheric pressure chemical vapor deposition of in-situ doped amorphous silicon layers for passivating contacts," 35th European Photovoltaic Solar Energy Conference and Exhibition, pp. 785-791 (2018).
- <http://unsworks.unsw.edu.au/fapi/datastream/unsworks:58583/SOURCE02?view=true> (accessed on 14-05-2021)
- Stodolny, M.K., Anker, J., Geerligs, B.L., Janssen, G.J., Van De Loo, B.W., Melskens, J., Santbergen, R., Isabella, O., Schmitz, J., Lenes, M., Luchies, J.M., "Material properties of LPCVD processed n-type polysilicon passivating contacts and its application in PERPoly industrial bifacial solar cells," *Energy Procedia*, Vol. 124, pp. 635-642 (2017).
- Padhamnath, P., Wong, J., Nagarajan, B., Buatis, J.K., Ortega, L.M., Nandakumar, N., Khanna, A., Shanmugam, V., Duttagupta, S., "Metal contact recombination in monoPoly™ solar cells with screen-printed & fire-through contacts," *Solar Energy Materials and Solar Cells*, Vol. 192, pp. 109-116 (2019).
- Feldmann, F., Reichel, C., Müller, R., Hermle, M., "The application of poly-Si/SiO_x contacts as passivated top/rear contacts in Si solar cells," *Solar Energy Materials and Solar Cells*, Vol. 159, pp. 265-271 (2017).
- Mekhilef, S., Safari, A., Mustaffa, W.E.S., Saidur, R., Omar, R., Younis, M.A.A., "Solar energy in Malaysia: Current state and prospects," *Renewable and Sustainable Energy Reviews*, Vol. 16, No. 1, pp. 386-396 (2012).
- Chen, D., Chen, Y., Wang, Z., Gong, J., Liu, C., Zou, Y., He, Y., Wang, Y., Yuan, L., Lin, W., Xia, R., "24.58% total area efficiency of screen-printed, large area industrial silicon solar cells with the tunnel oxide passivated contacts (i-TOPCon)

- design,” *Solar Energy Materials and Solar Cells*, Vol. 206, pp. 110258:1-8 (2020).
18. Chen, Y., Chen, D., Liu, C., Wang, Z., Zou, Y., He, Y., Wang, Y., Yuan, L., Gong, J., Lin, W., Zhang, X., “Mass production of industrial tunnel oxide passivated contacts (i-TOPCon) silicon solar cells with average efficiency over 23% and modules over 345 W,” *Progress in Photovoltaics: Research and Applications*, Vol. 27, No. 10, pp. 827-834 (2019).
 19. Römer, U., Peibst, R., Ohrdes, T., Lim, B., Krügener, J., Bugiel, E., Wietler, T., Brendel, R., “Recombination behavior and contact resistance of n+ and p+ poly-crystalline Si/mono-crystalline Si junctions,” *Solar Energy Materials and Solar Cells*, Vol. 131, pp. 85-91 (2014).
 20. Yan, D., Cuevas, A., Bullock, J., Wan, Y., Samundsett, C., “Phosphorus-diffused polysilicon contacts for solar cells,” *Solar Energy Materials and Solar Cells*, Vol. 142, pp. 75-82 (2015).
 21. Rohatgi, A., Zimbardi, F., Rounsaville, B., Benick, J., Stradins, P., Norman, A., Lee, B., Upadhyaya, A., Ok, Y.W., Tao, Y., Tam, A., “Overcoming the Fundamental Bottlenecks to a new world-record silicon solar cell. Final Technical Report (No. DOE-GT-6336),” Georgia Inst. of Technology, Atlanta, GA (United States) (2017).
 22. Green, M.A., Dunlop, E.D., Hohl-Ebinger, J., Yoshita, M., Kopidakis, N., Ho-Baillie, A.W., “Solar cell efficiency tables (Version 55),” *Progress in Photovoltaics: Research and Applications*, Vol. 28, No. 1, pp. 3-15 (2020).
 23. Younis, I.M., “Cost benefit analysis of photovoltaic technology adoption at rest and service area for malaysia highway,” Doctoral dissertation, Universiti Teknologi Malaysia (2019).
 24. Lauinger, T., Schmidt, J., Aberle, A.G., Hezel, R., “Record low surface recombination velocities on 1 Ω cm p-silicon using remote plasma silicon nitride passivation,” *Applied Physics Letters*, Vol. 68, No. 9, pp. 1232-1234 (1996).
 25. Grant, N.E., Markevich, V.P., Mullins, J., Peaker, A.R., Rougieux, F., Macdonald, D., Murphy, J.D., “Permanent annihilation of thermally activated defects which limit the lifetime of float-zone silicon,” *Physica status solidi (a)*, Vol. 213, No. 11, pp. 2844-2849 (2016).
 26. Feldmann, F., Steinhauser, B., Arya, V., Büchler, A., Brand, A.A., Kluska, S., Hermle, M., Glunz, S.W., “Evaluation of TOPCon technology on large area solar cells,” 33rd European Photovoltaic Solar Energy Conference Exhibition, pp. 1-3 (2017).
 27. Lindekugel, S., Lautenschlager, H., Ruof, T., Reber, S., “Plasma hydrogen passivation for crystalline silicon thin-films,” 23rd European Photovoltaic Solar Energy Conference, pp. 2232-2235 (2008).
 28. Richter, A., Glunz, S.W., Werner, F., Schmidt, J., Cuevas, A., “Improved quantitative description of Auger recombination in crystalline silicon,” *Physical Review B*, Vol. 86, No. 16, pp. 165202:1-14 (2012).
 29. Feldmann, F., Fellmeth, T., Steinhauser, B., Nagel, H., Ourinson, D., Mack, S., Lohmüller, E., Polzin, J.I., Benick, J., Richter, A., Moldovan, A., “Large area TOPCon cells realized by a PECVD tube process,” 36th European Photovoltaic Solar Energy Conference and Exhibition (2019).
 30. <https://www.infolink-group.com/en/solar/analysis-trends/N-type-technology> (accessed on 14-05-2021)
 31. <https://www.energytrend.com/research/20210105-20519.html> (accessed on 14-05-2021)
 32. Richter, A., Müller, R., Benick, J., Feldmann, F., Steinhauser, B., Reichel, C., Fell, A., Bivour, M., Hermle, M., Glunz, S.W., “Design rules for high-efficiency both-sides-contacted silicon solar cells with balanced charge carrier transport and recombination losses,” *Nature Energy*, pp. 1-10 (2021).
 33. Park, C., Balaji, N., Ahn, S., Park, J., Cho, E.C., Yi, J., “Effects of tunneling oxide defect density and inter-diffused carrier concentration on carrier selective contact solar cell performance: Illumination and temperature effects,” *Solar Energy*, Vol. 211, pp. 62-73 (2020).